J Membrane Biol (2010) 237:115–123
DOI 10.1007/s00232-010-9312-z

Epithelial Barrier Resistance is Increased by the Divalent Cation Zinc in Cultured MDCKII Epithelial Monolayers

Georgina Carr · Jamie A. Wright · Nicholas L. Simmons

Received: 20 September 2010 / Accepted: 20 October 2010 / Published online: 6 November 2010

Abstract Topical zinc applications promote wound healing and epithelialization. "Leaky" MDCKII epithelia exposed to apical $ZnCl_2$ (10 mM) showed a time-dependent increase ($t_{0.5}$ 22.2 ± 2.7 min) of transepithelial resistance (R_t) from 82.3 ± 2.4 Ω cm^2 to 1,551 ± 225.6 Ω cm^2; the increase was dose-dependent, being observed at 3 mM but not at 1 mM. Basal Zn^{2+} applications also increased epithelial resistance (at 10 mM to 323 ± 225.6 Ω cm^2). The linear current–voltage relationship in control epithelia changed after apical 10 mM $ZnCl_2$ to show rectification. Voltage deflections resulting from inward currents showed time-dependent relaxation (basal potential difference (p.d.)-positive), with outward currents being time-independent. Cation selectivity was tested after apical $ZnCl_2$ elevated resistance; both the NaCl:mannitol (basal replacement) dilution p.d. and the choline:Na bi-ionic p.d. decreased (P_{Na}/P_{Cl} from 4.9 to 2.3 and $P_{Na}/P_{choline}$ from 3.8 to 2.1, respectively). Transepithelial paracellular basal to apical ^{45}Ca fluxes increased approximately twofold when driven by a basal positive Na:NMDG bi-ionic p.d., but with basal 10 mM $ZnCl_2$, ^{45}Ca fluxes decreased approximately twofold. Neither ZO-1 nor occludin distribution was altered after ~2-h exposure to apical 10 mM $ZnCl_2$. However, claudin-2, though present at the tight junction, increased within the cell. Increased epithelial barrier resistance by Zn^{2+} is due to modification of the paracellular pathway, most probably by multiple mechanisms.

G. Carr · J. A. Wright · N. L. Simmons (✉)
Epithelial Research Group, ICAMB, Medical School, University of Newcastle upon Tyne, Framlington Place, Newcastle upon Tyne NE2 4HH, UK
e-mail: n.l.simmons@ncl.ac.uk

Keywords Tight junction · Madin-Darby canine kidney cell · Zinc · Paracellular pathway · Block

Introduction

Topical zinc applications provide the therapeutic benefit of accelerated wound healing, with clinical evidence suggesting roles in autodebridgement, epithelial restitution and antimicrobial actions (Lansdown et al. 2007). Zinc oxide paste in dressing and bandages provides a depot for bioavailable zinc concentrations, with constant levels of 1–3 mM being achieved that are nontoxic but high enough to promote wound healing (Lansdown et al. 2007). Recent studies have shown that extracellular Zn^{2+} applied or released from injured tissue may act via a zinc receptor (GPR39) and MAP kinase activation, leading to keratinocyte migration and epithelial wound repair (Sharir et al. 2010).

Zinc is also implicated in modification of epithelial barrier function in both renal and intestinal epithelia; zinc protects renal function during cadmium toxicity, preventing cadmium-induced change in claudin expression (Jacquillet et al. 2006). Recent studies in intestinal epithelia have shown that long-term depletion of zinc results in increased paracellular conductance associated with alteration of junctional proteins including ZO-1 and claudin-1 (Zhong et al. 2010). A recent meta-analysis of 13 separate studies (Lukacik et al. 2008) has confirmed the long-standing observation (Roy et al. 1992) that oral zinc supplementation decreases the severity and duration of diarrhea in humans. Although the mechanism(s) is still uncertain, both direct and indirect actions of zinc on the intestinal epithelium have been suggested (Crane et al. 2007; Hoque et al. 2009; Roselli et al. 2003). Tight junctional permeability assessed

directly by lanthanum penetration across intestinal tight junctions was decreased by zinc in an experimental model of colitis (Sturniolo et al. 2002).

In our own studies of a renal inner medullary cell line (mIMCD-3) (Linley et al. 2009) we identified in whole-cell patch-clamp studies that extracellular zinc raised intracellular Ca^{2+}, stimulating a calcium-activated Cl^- conductance. In order to extend whole-cell studies to the intact epithelium, we tested the effect of extracellular zinc in reconstituted epithelial monolayers. Although significant activation of electrogenic transepithelial ion transport was not observed, higher concentrations of zinc appeared to result in a time-dependent increase in epithelial resistance (decrease in epithelial conductance). This unexpected result prompted us to ask whether zinc could modify paracellular transport more generally. In the present report we examined whether in the extensively characterized model "leaky" epithelium, MDCKII (Cereijido et al. 1978; Furuse et al. 2001; Richardson et al. 1981) a direct action of zinc on the tight junction/paracellular pathway could be established. We show that Zn^{2+} has a major effect on the MDCKII paracellular pathway, converting it to a high resistance similar to that in "tight" epithelia. We suggest that Zn^{2+} action to increase epithelial barrier resistance is an additional feature to its action in promoting epithelial restitution after insult.

Materials and Methods

Cell Culture

MDCKII cells (passages 114–120) (Richardson et al. 1981) were serially cultured in Eagle modified essential medium (EMEM), supplemented with fetal calf serum (10% v/v), glutamine (1% v/v, final concentration 2 mM) and an antibiotic mix of penicillin–streptomycin (100 U/ml, 100 µg/ml, respectively). mIMCD-3 cells (Linley et al. 2009) were grown in 75-cm^2 Roux flasks without antibiotics in Ham's F12 and DMEM (50/50 v/v%) with 1 g/l glucose, 10% fetal calf serum and 2 mM L-glutamine at 37°C in humidified air:5% CO_2 (Linley et al. 2009). Epithelial layers of MDCKII/mIMCD-3 cells were prepared by seeding onto 12-well culture inserts (Snapwell 3407 or Transwell 3401 [MDCK only], 12 mm diameter, 0.4 µm pore size, 1.14 cm^2 growth area uncoated polycarbonate filters; Costar, Corning BV, Amsterdam, Holland) at high density (5×10^5 cells cm^{-2}). Cells were maintained at 37°C in a humidified incubator with 5% CO_2 in air for 5 days without medium replacement prior to use in experiments. Routine monitoring of transepithelial resistance to assess confluence was made using an Evometer (World Precision Instruments, Stevenage, UK).

Solutions

A modified Krebs solution was used for electrical measurements of epithelial layers and measurement of transepithelial fluxes (all mmol/l): NaCl 137, KCl 5.4, $CaCl_2$ 2.8, $MgSO_4$ 1.0, NaH_2PO_4 0.3, KH_2PO_4 0.3, glucose 10, HEPES/Tris 15 (pH 7.4, 37°C). For measurements of bi-ionic/dilution potentials elicited across the cation-selective paracellular pathway of MDCKII epithelia, equimolar substitutions of NaCl were made using *N*-methyl D-glucamine Cl, choline Cl or mannitol (274 mM).

Electrophysiological Experiments

MDCKII/mIMCD-3 epithelial layers grown on Snapwells were mounted in modified Ussing chambers (Costar Corning, Lowell, MA), maintained at 37°C connected to an automatic voltage/current clamp (DVC-1000; World Precision Instruments, New Haven, CT). Saturated 3 M KCL-agar bridges were used to connect reversible electrodes (calomel for potential difference (p.d.), [mV] measurements and Ag/AgCl for current passage). Asymmetry in the p.d. arising from the calomel/agar bridges was zeroed prior to tissue mounting. Correction for voltage drop across the series fluid resistance upon current passage was made in assembled chambers prior to chamber assembly with Snapwells. Correction for junction potentials with asymmetric solutions ($V_{ef} - V_f$) was made using measurements of p.d. generated using cell-free Snapwells in Ussing chambers corrected for the diffusion potential across the filter (V_{ef}) and calculated values of NaCl dilution or bi-ionic potentials (V_f) (Ng and Barry 1995; Yu et al. 2009). Relative ionic permeabilities were calculated using the Goldman equation (Hille 1972). Measurements of open-circuit electrical potential difference and transepithelial resistance (R_t) were made by excursions of the clamp in voltage/current clamp modes; all data were recorded continuously using PowerLab software (ADI Instruments, Chalgrove, UK). Measurements of R_t were corrected for filter resistance (typically 76 Ω cm^2).

As an alternative, Transwell-grown MDCKII epithelia were assembled into individual chambers of the CellZscope maintained at 37°C (NanoAnalytics, Münster, Germany) for measurement of epithelial resistance (R_t) and capacitance (C_t). In these experiments monolayer integrity was confirmed prior to experimentation by measurement of Na:NMDG bionic p.d. (see below). R_t and C_t were determined from fitting the impedance spectrum (1–10^5 Hz) of individual determinations to a five-parameter equivalent circuit model incorporating R_t, C_t and a constant phase element representing the bathing solutions (NanoAnalytics). Since each impedance spectrum required ~40 s to capture, continuous determination of R_t was achieved using Snapwell/Ussing chambers (see above).

Transepithelial ^{45}Ca Flux Measurements

Epithelial layers were washed (four times) in modified Krebs buffer and placed in 12-well plates, and 0.5 ml of modified Krebs buffer were added to apical and 1.0 ml to basal chambers for 10 min at 37°C. Monolayer integrity and paracellular cation selectivity were then tested by transfer of the cell layers to 12-well plates containing the NMDG-Krebs and measurement of the resulting bi-ionic p.d. (40.0 ± 1.3 mV basal solution electropositive, $n = 12$) (Carr et al. 2006). Epithelial layers were then replaced in normal Krebs solutions. Radiolabeled ^{45}Ca (0.5 μCi/ml, NEZ013, 370 GBq/g; New England Nuclear, Boston, MA) was then added to the basolateral chamber with equal concentrations of 2.8 mM unlabeled Ca present in both apical and basal chambers. The use of such concentrations (low specific activity) minimizes transcellular radiolabeled flux. Fluxes in the secretory (basal to apical, J_{b-a}) direction were determined to also minimize the contribution from transcellular (absorptive) fluxes. Fluxes were then measured in three consecutive periods of 1 h so that the effects of transepithelial voltage imposition could be assessed in a paired manner on individual cell monolayers. Apical samples were 0.1 ml with replacement. In the second period epithelial layers were transferred to 12-well plates containing 1.0 ml of ^{45}Ca NMDG-Krebs solution to provide an electrical driving force across the epithelium (Carr et al. 2006). Finally, transfer to 12-way plates containing ^{45}Ca-Krebs allowed an additional control period in the absence of the imposed electrical gradient to be measured. Samples of ^{45}Ca-Krebs/NMDG Krebs were also taken. ^{45}Ca activities were determined by liquid scintillation spectrometry. All fluxes are expressed as moles per centimeter squared per hour.

Confocal Microscopy

Control and treated MDCKII cell monolayers were washed in Krebs, fixed and permeabilized in methanol at 0°C for 15 min and then stored overnight in phosphate-buffered saline (PBS) at 4°C. Cell layers were washed again, overlaid on 3% horse serum in PBS at room temperature for 1 h and then incubated overnight at 4°C with primary antibody (typically diluted 1:100 in 3% horse serum in PBS). The antibodies used were anti-occludin, a mouse monoclonal against an undefined epitope within 150 amino acids of the C terminus of human occludin, showing canine cross-reactivity; anti-claudin-2, a rabbit polyclonal against the C terminus of human claudin-2, showing canine cross-reactivity; and anti-ZO-1, a mouse monoclonal against amino acids 334–634 of the human ZO-1 protein, also displaying canine cross-reactivity. All primary antibodies were purchased from Invitrogen (Carlsbad, CA). Monolayers were then washed three times and incubated for 1 h at room temperature in 3% donkey serum in PBS prior to incubation with an appropriate Alexa Fluor conjugated secondary antibody (Molecular Probes, Eugene, OR). Typically, monolayers were then washed three times in PBS and counterstained with propidium iodide (Molecular Probes) to label nuclei. Immunofluorescence was detected by confocal laser scanning microscopy (TCS NT confocal microscope; Leica, Cambridge, UK).

Statistics

Data are expressed as mean values ± SEM for n separate epithelial layers. Significance of difference between mean values was determined using ANOVA with Bonferroni corrections for multiple comparisons applied to Student's t-test (unpaired data) or t-tests between individual data pairs (where appropriate). For data that did not display a normal distribution, a Kruskal-Wallis ANOVA on ranks was performed with multiple comparisons for significance performed by Dunn's method or by Mann-Whitney U by rank between individual data pairs. The level of significance was set at $P \leq 0.05$.

Results

Epithelial monolayers of mIMCD-3 reconstitute with a transepithelial resistance (R_t) of $151 \pm 22.7\ \Omega\ cm^2$ ($n = 9$). We initially sought to test the effect of extracellular applications of $ZnCl_2$ since 400 μM Zn^{2+} activated a Cl^- conductance (Linley et al. 2009). No effect on short-circuit current consistent with Cl^- secretion was evident in this cell line with apical Zn^{2+}, but at more elevated levels of Zn^{2+} an increased R_t was observed. With 10 mM apical $ZnCl_2$, R_t increased to $967 \pm 344\ \Omega\ cm^2$ ($n = 9$, $P < 0.01$, paired signed rank test). Since mIMCD-3 paracellular pathways are poorly characterized, we chose MDCKII epithelial monolayers for further study.

MDCKII layers (CellZscope measurements) in Krebs buffer exposed to apical $ZnCl_2$ at 10 mM showed a sustained rise in R_t from control levels ($82.3 \pm 2.4\ \Omega\ cm^2$) to those typical of a high-resistance tight epithelium ($1{,}551 \pm 225.6\ \Omega\ cm^2$, $P < 0.001$, Mann-Whitney U) (Fig. 1A, B). Since MDCKII epithelial conductance is dominated by the paracellular pathway (Cereijido et al. 1978; Gitter et al. 1997; Lo et al. 1995), the decrease in epithelial conductance from 12 to 0.6 mS cm^{-2} (~95% reduction) indicates that the site of action of Zn^{2+} is the paracellular pathway. In order to test whether Zn^{2+} was effective from both sides of the paracellular pathway, 10 mM $ZnCl_2$ was applied to the basolateral cell surface; R_t was also increased, but peak values were later and smaller than those achieved with

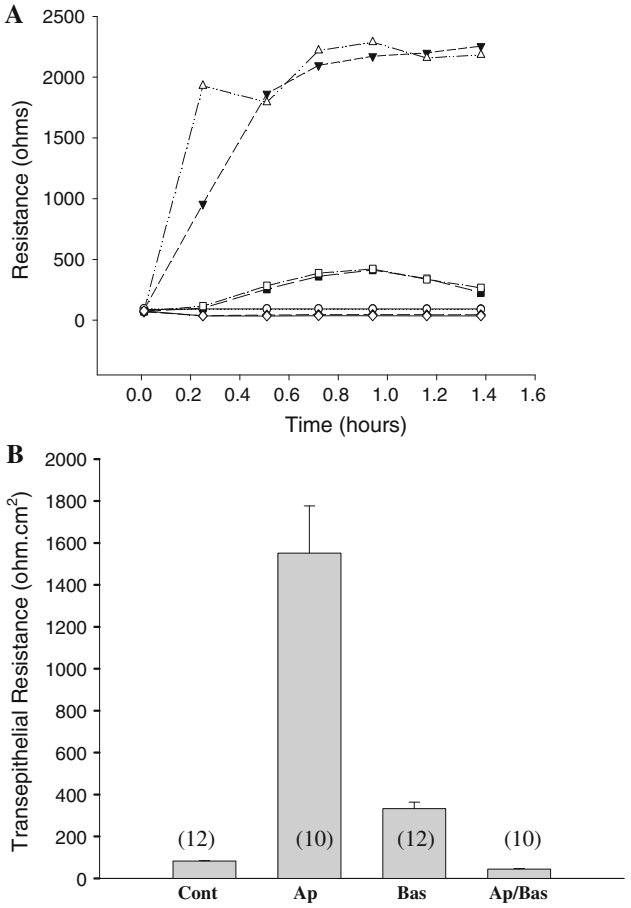

Fig. 1 Action of Zn on transepithelial resistance (R_t) of MDCKII monolayers. **A** Time course of change for individual monolayers, showing difference between apical (*open and filled triangles*), basal (*open and filled squares*), dual addition of 10 mM $ZnCl_2$ to apical/basal bathing solutions (*open diamonds*) and controls (*open circles*). **B** Mean data for R_t at 2 h, $n = 10/12$ monolayers, ±SEM

apical application (to 323 ± 225.6 Ω cm^2, $P < 0.001$, Mann-Whitney U vs. controls) (Fig. 1A, B). Addition of 10 mM $ZnCl_2$ to both apical and basal solutions resulted in a decrease in R_t to 44.4 ± 1.9 Ω cm^2 ($P < 0.001$ vs. controls) (Fig. 1B).

The action of $ZnCl_2$ to increase R_t with unilateral exposure was observed in two other measurement systems: in Transwell-grown MDCKII monolayers measured in situ with Evometer chopstick electrodes and in Snapwell-grown MDCKII monolayers mounted in Ussing chambers. For Transwell-grown MDCKII epithelial monolayers with apical addition of 10 mM $ZnCl_2$, resistance increased from 210 ± 7 Ω cm^2 (all $n = 3$) to 2,334 ± 175 Ω cm^2 at 90-min incubation ($P < 0.001$), while with 3 mM apical addition the increment was smaller at 450 ± 33 Ω cm^2. Applications of 1 mM gave 207 ± 9 Ω cm^2 (NS). A similar pattern was observed for basal additions of $ZnCl_2$; from control values of 154 ± 6 Ω cm^2 (all $n = 3$) R_t increased to 587 ± 20 Ω cm^2 at 90-min incubation ($P < 0.001$), while with 3 mM apical addition the increment was smaller at 393 ± 20 Ω cm^2. Applications of 1 mM were without effect, 154 ± 6 Ω cm^2 (NS). Note that control epithelial layers contained 50 mM mannitol to control for any osmotic effects of $ZnCl_2$ addition; R_t minus mannitol was 150 ± 3 Ω cm^2 or 107 ± 3 Ω cm^2 for apical/basal layers prior to mannitol addition. The increased R_t plus apical or basal $ZnCl_2$ was reversed by washing; after 5 min R_t had decreased from 2,311 ± 217 Ω cm^2 ($n = 3$) to 118 ± 8 or 585 ± 23 Ω cm^2 ($n = 3$) to 180 ± 1 Ω cm^2, respectively.

Since CellZscope measurements do not allow detailed time-resolved measurements of the increase in resistance, a detailed time course was obtained using Snapwell-grown MDCKII layers in Ussing chambers. Figure 2A shows that Zn^{2+} addition did not stimulate any change in transepithelial p.d. (no baseline change), as would be expected if transcellular transport was altered; instead, there was a slow increase in R_t with a $t_{0.5}$ of 22.2 ± 2.7 ($n = 7$) min. The decrease in epithelial conductance ($1/R_t$) approximates only a single exponential (Fig. 2B), indicating that a simple one-site action of Zn^{2+} is unlikely. Figure 3 shows current–voltage plots for epithelial layers in the presence or absence of Zn^{2+}; for controls, square-wave excursions of the clamping transepithelial current in the range ±250 μA in 50-μamp steps gave a linear current–voltage relationship (Fig. 3B), with voltage deflections showing no time dependence (Fig. 3B). In contrast, after prolonged application of apical 10 mM $ZnCl_2$ to achieve the steady-state resistance increase, the current–voltage relationship was markedly nonlinear, outward (–) currents generating a basal negative transepithelial p.d. giving rise to a conductance calculated at 0–200 μA of 1.18 ± 0.28 mS cm^{-2} ($n = 4$), which was smaller than that seen for inward currents, 0–200 μA of 2.52 ± 0.39 mS cm^{-2} ($n = 4$). In addition to the rectifying current–voltage relationship, inward current excursions plus apical $ZnCl_2$ showed time-dependent relaxation of voltage (basal p.d.-positive); in contrast, outward current excursions were relatively time-independent (Fig. 3C). On application of $ZnCl_2$ to the basal bathing solution, both the rectification and kinetic profile were reversed (Fig. 3D); in this case, outward current excursions plus basal $ZnCl_2$ now showed marked kinetics with time-dependent relaxation of voltage (basal p.d.-negative), while inward current excursions were relatively time-independent (Fig. 3D). This behavior is consistent with a voltage-dependent block of the paracellular cation-selective pore (Tsien et al. 1987).

We also investigated the permselectivity of the paracellular pathway after 90-min incubation with apical $ZnCl_2$, at which time the increase in R_t had reached a plateau; the NaCl:mannitol (basal replacement) dilution p.d. decreased from 38.1 ± 2.6 mV (basal solution electropositive) to 20.1 ± 1.1 mV ($n = 7$) (P_{Na}/P_{Cl} from 4.9 to

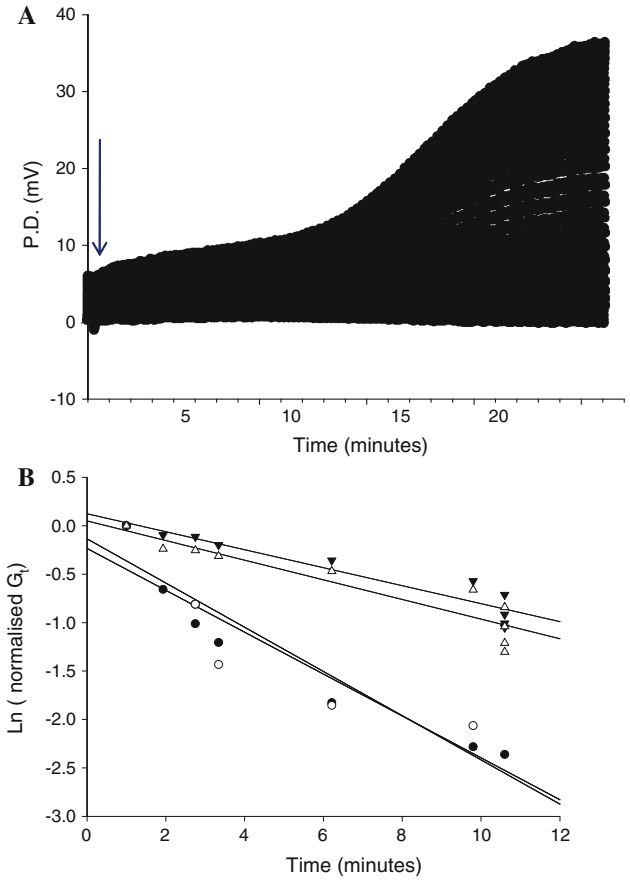

Fig. 2 Time-resolved increase in R_t in MDCKII. **A** Original record of MDCKII monolayer mounted in Ussing chamber and subjected to excursions of the current clamp between 0 and 30 μA; orientation of p.d. basal solution electropositive. *Arrow* $ZnCl_2$, 10 mM, added to the apical bathing medium. **B** Semi-log plot of the normalized decrease in epithelial conductance ($G_t = 1/R_t$) vs. time for four individual MDCKII monolayers. *Solid lines* represent the linear regression line for each monolayer

2.3) and the choline:Na bi-ionic p.d decreased from 32.0 ± 2.7 to 18.0 ± 1.3 mV ($P_{Na}/P_{choline}$ from 3.8 to 2.1). Therefore, the overall cation selectivity of the paracellular pathway was decreased.

In order to verify blockade of the paracellular pore by unilateral application of $ZnCl_2$ by an independent method, we characterized voltage-dependent ^{45}Ca fluxes. The paracellular pathway is a major route for divalent cation permeation (Wright and Diamond 1968), with calcium and magnesium fluxes across the paracellular pathway being the major routes for absorption in thick ascending limbs of the kidney (Blanchard et al. 2001). We have previously described a method (Carr et al. 2006) to identify paracellular flux of a cationic solute by imposing a transepithelial p.d. in the absence of external current passage by establishing a bi-ionic p.d. dependent on the Na gradient. Figure 4 shows that basal to apical ^{45}Ca flux was increased approximately twofold in the presence of an Na:NMDG-mediated p.d., and this was fully reversed on return to control conditions; in contrast, in the presence of basal $ZnCl_2$, ^{45}Ca flux was decreased approximately twofold compared to controls despite the presence of the Na:NMDG-mediated p.d. Therefore, comparing ^{45}Ca flux driven by the imposed p.d. in the presence and absence of Zn^{2+}, it is clear that unilateral application of Zn^{2+} prevents cation movement via the paracellular pathway.

Finally, we asked whether unilateral (apical) $ZnCl_2$ treatment was associated with structural change within the tight junction as represented by protein content or distribution. As can be seen from Figure 5, there was no discernible change in the distribution of either ZO-1 or occludin on ~2-h exposure to apical 10 mM $ZnCl_2$. However, it is noteworthy that a fraction of claudin-2 was delocalized from the tight junctions and was present in an intracellular perinuclear compartment after Zn^{2+} exposure, suggesting an increased turnover and internalization of claudin-2 from the tight junction.

Discussion

The data presented here show that application of Zn^{2+} to the apical surface of MDCKII epithelia has a profound effect on increasing the barrier resistance, values at steady-state approaching those typical of "tight" epithelia.

Since the pioneering work of Fromter, Wright and Diamond (Fromter 1972; Fromter and Diamond 1972; Wright and Diamond 1968), it has been known that differences between "tight" and "leaky" epithelia result mainly from differences in the resistance of the paracellular pathway between epithelial cells rather than the high-resistance transcellular pathway. In leaky epithelia, such as rabbit gallbladder and small intestine, the paracellular pathway consists of conductive water-filled channels/pores lined by ionizable acidic groups that render them cation-selective. On the basis of molecular studies, the important protein components of such tight junctions are claudin family members (Anderson and Van Itallie 2009). Of special importance in examining structure–function studies has been the use of high- and low-resistance MDCK cell lines in which claudin expression has been manipulated (Colegio et al. 2003; Furuse et al. 2001; Stevenson et al. 1988; Yu et al. 2009). MDCKII epithelia are typical leaky epithelia, where impedance analysis and voltage scanning studies have confirmed the paracellular pathway as the location of the majority (>80%) of the transepithelial conductance (Gitter et al. 1997; Lo et al. 1995). Expression of claudin-2 results in the formation of cation-selective pores in leaky epithelia and transforms tight epithelia to leaky (Furuse et al. 2001; Yu et al. 2009). Claudins are tetraspan membrane proteins with two extracellular loops that project and must span the space

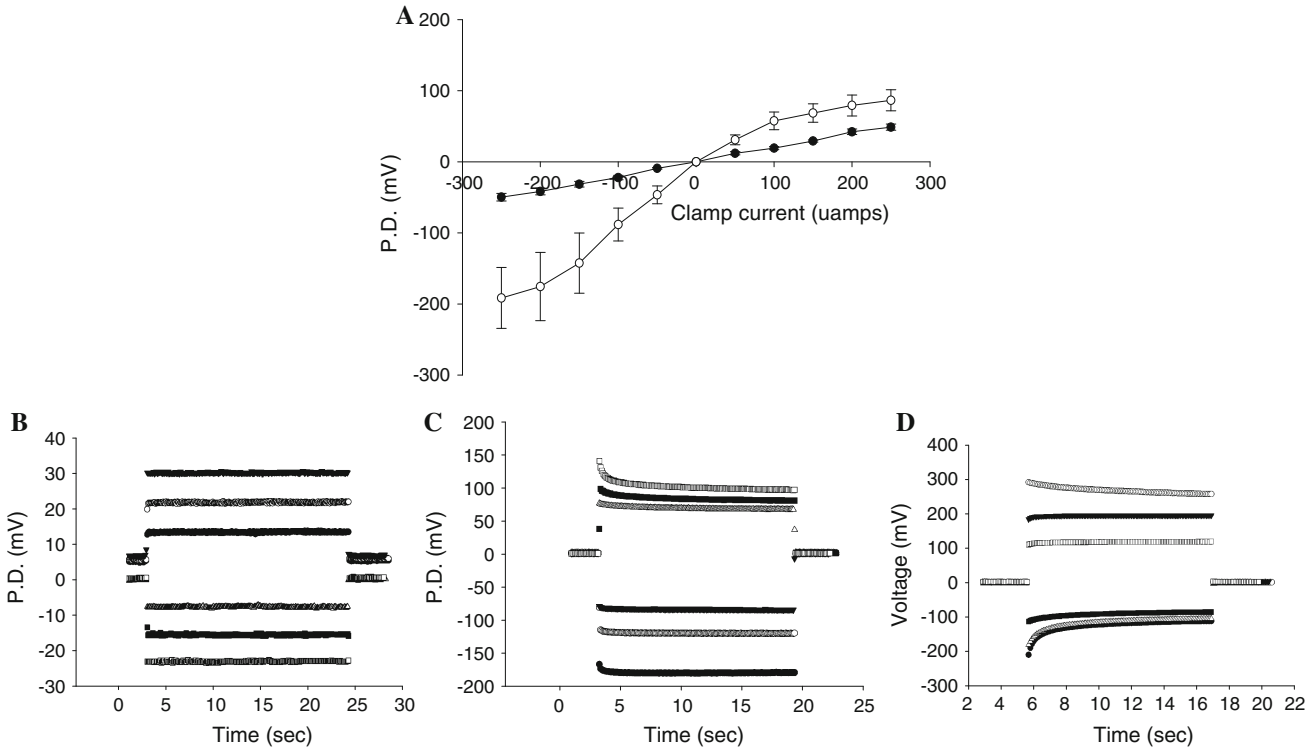

Fig. 3 **A** Action of apical $ZnCl_2$ (10 mM) on the voltage–current relationship of MDCKII epithelial layers; control epithelia (*solid circles*), with apical $ZnCl_2$ (*open circles*), application at steady state after resistance increase and 10 s after current pulse application. Data are the mean ± SEM of four separate epithelial layers; error bars lie within points if not shown. Polarity of p.d. relates to the basal bathing solution (apical solution grounded). **B–D** Voltage deflections to current clamp square-wave excursions of ±100, 150 and 200 μA in individual epithelial monolayers (**B**), control monolayer (**C**), with apical application of 10 mM $ZnCl_2$ (**D**) from a separate experiment, with basal application of $ZnCl_2$

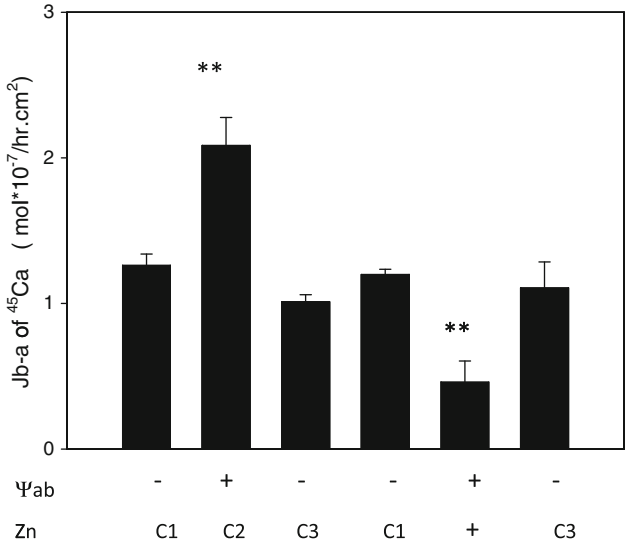

Fig. 4 Effect of an imposed transepithelial p.d. and Zn^{2+} on transepithelial ^{45}Ca fluxes. Basal to apical transepithelial ^{45}Ca flux (J_{b-a}) was determined in three consecutive 1-h periods (C1–3); in the second period (C2/+) an apical to basal Na gradient imposes a basal solution electropositive p.d. across the epithelium in either control layers or layers with 10 mM $ZnCl_2$ (+) in the basal bathing solution. A final control period is without an imposed p.d. or Zn^{2+} treatment (C3)

between the two adjacent membranes from adjoining cells that form the tight junction complex (Tsukita and Furuse 2002). Of the two extracellular claudin domains, domain 1 has been shown to contain key acidic amino acids that determine the cation selectivity of the pore (Colegio et al. 2003; Van Itallie et al. 2003; Yu et al. 2009). Domain 2, though containing conserved acidic residues, must be involved in some way in the formation and stabilization of the interaction of proteins across the tight junction cleft (Anderson and Van Itallie 2009).

There are two main possibilities as to the action of extracellular zinc. First, the effect could be indirect, by Zn^{2+} activating an intracellular signaling cascade to alter the properties of the tight junction. Activation of the EGFR via the membrane-bound HB-EGF ligand (Singh et al. 2007) results in a long-term increase in R_t, which is associated with a reduction of claudin-2 expression within the tight junction. Chronic acidification also leads to reduction of claudin-2 and increased resistance in MDCKII cells (Balkovetz et al. 2009). The partial cellular redistribution of claudin-2 by Zn^{2+} observed in the present data could indicate that this may, in part, explain the increase in resistance observed. However, claudin-2 is still present in cell junctions after

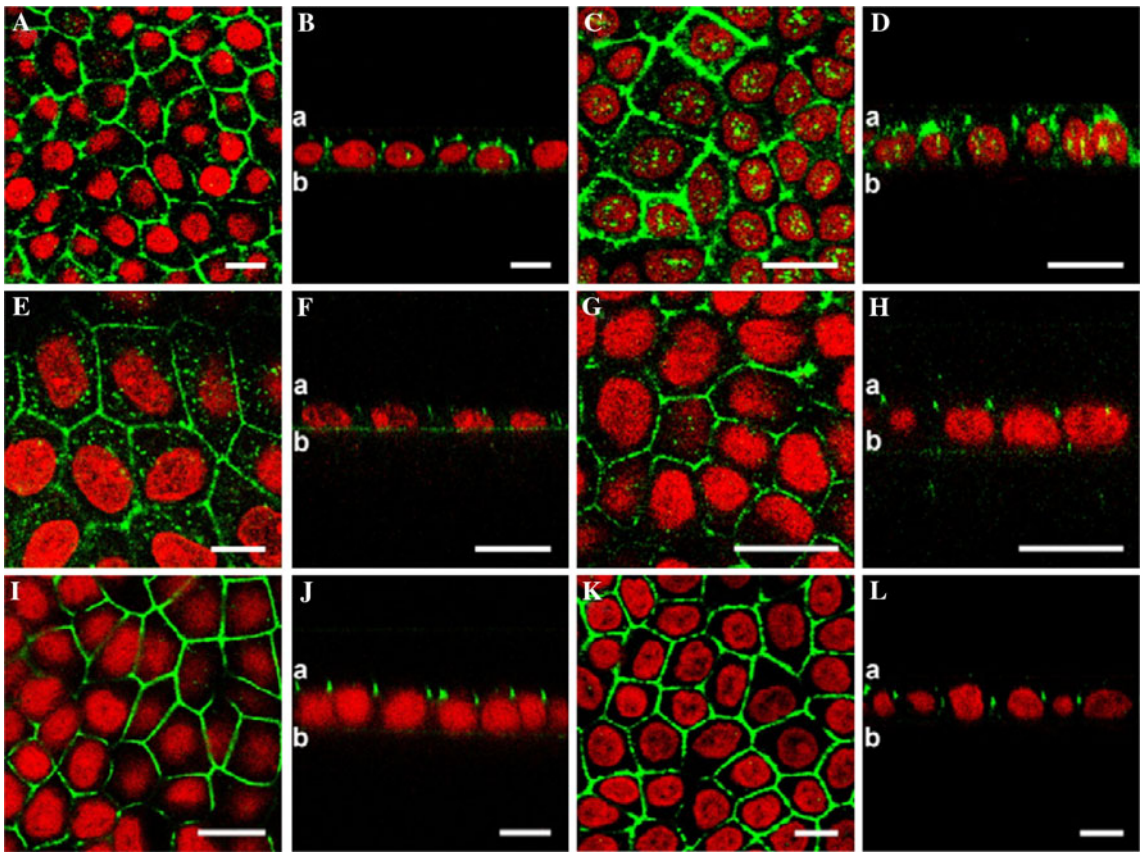

Fig. 5 Action of apical $ZnCl_2$ (10 mM) at 2 h on junctional protein distribution. **A**, **B** Control monolayer immunofluorescence for claudin-2, *xy* (en-face view) and *xz* sections, respectively. **C**, **D** Zinc-treated monolayer, immunofluoresence for claudin-2, *xy* and *xz* views. **E**, **F** Control monolayer immunofluorescence for occludin, *xy* and *xz* views. **G**, **H** Zinc-treated monolayer immunofluorescence for occludin, *xy* and *xz* views. **I**, **J** Control monolayer immunofluorescence for ZO-1, *xy* and *xz* views. **K**, **L** Zinc-treated monolayer immunoflourescence for ZO-1, *xy* and *xz* views. *a* apical, *b* basolateral. Scale bars = 10 μm

Zn^{2+}, and it is clear that the dynamic behavior of ZO-1 and occludin in traffic between intracellular vesicles and the tight junction is much more rapid than that of claudins, which show extended retention within the tight junction and a low turnover rate (Shen et al. 2008). Though we cannot exclude such indirect cellular actions, the alternative is a direct action of Zn^{2+} within the paracellular pathway.

Tang and Goodenough (2003) have emphasized the pore-like behavior of the tight junction paracellular pathway in leaky epithelial cells, describing its similarity to plasma membrane ion channels with respect to selectivity, molecular size discrimination, concentration dependence of ion permeabilities, competition between permeant ions, anomalous mole-fraction behavior and pH sensitivity. An additional feature of conventional ion channels is the voltage-dependent channel block by divalent cations (Tsien et al. 1987); indeed, divalent cations such as zinc have been reported to block epithelial Na channels and so prove to be useful probes of channel function (Amuzescu et al. 2003).

We propose therefore that Zn^{2+} acts to block the paracellular pore. Evidence for this is that unilateral block of the paracellular pore shows a clear voltage dependence for both the current–voltage relationship and the time-dependent relaxation of voltage with outward current on apical application (and vice versa on basal application of Zn^{2+}). This finding suggests that Zn^{2+} may enter the paracellular pore but traverse it only slowly since block is not relieved by negative or positive transepithelial p.d. but only by positive p.d. for apical application and negative p.d. for basal application (Tsien et al. 1987). The apparent low affinity of zinc action may suggest that access of the larger hydrated divalent cation to the paracellular pore, compared to sodium, is restricted by the pore size and the relative field strengths of acidic residues (e.g., Asp68) and the hydrated zinc cation.

Few studies have used soluble probe molecules to address the nature of the leaky paracellular pathway. The studies of Moreno (1975) identified 2,4,6-triaminopyrimidine and a variety of other pyrimidine derivatives as such probes, in that their molecular size suggested they would gain access to the paracellular channel and their strong H-bond proton donor ability would allow them to interact

with acidic groups within the channel. 2,4,6-Triaminopyrimidine specifically reduces conductance (increases resistance) in gallbladder epithelium by reducing Na conductance. Resistance increased from ~100 to 260 Ω cm^2. Importantly, block of the paracellular pathway by 2,4,6-triaminopyrimidine also reduced the cation selectivity of the junctional route as measured by dilution and bi-ionic p.d. elicited across the epithelium. 2,4,6-Triaminopyrimidine was rapidly effective at both epithelial surfaces ($t_{0.5}$ 10 s from the apical side, 130 s from the basal side), any disparity being explained by the diffusional differences imposed by the unstirred layers in the preparation (Moreno 1975). It is apparent that the time course of Zn^{2+} action on R_t is considerably slower than that of 2,4,6-triaminopyrimidine, with an extended $t_{0.5}$ of ~22 min after apical Zn^{2+} application. Zn^{2+} action is not symmetric; when applied from the basal surfaces, the resistance increase is attenuated and only peaks after 1 h of exposure. An additional feature of the response is the entirely different response of epithelial conductance to bilateral Zn^{2+} exposure; there is a sustained increase in epithelial conductance. In a similar manner to 2,4,6-triaminopyrimidine, Na:choline bi-ionic p.d. values are decreased compared to controls after 90 min. MDCK epithelia, however, retain overall cation selectivity after prolonged incubation despite a 95% reduction in conductance with apical Zn^{2+}. These observed differences between Zn^{2+} action within the paracellular pore and that of 2,4,6-triaminopyrimidine block in gallbladder suggest that a simple single-site binding model is unlikely.

It now seems that monovalent cation selectivity of the tight junction pore is derived from acidic residues present within the first extracellular domain (1) of claudins (e.g., claudin-2) (Van Itallie et al. 2003; Yu et al. 2009). It is also apparent from studies of mutated claudin-2 in high-resistance MDCK I epithelial monolayers that Asp68 contributes the important carboxylic acidic group to the selectivity filter (Yu et al. 2009). The second extracellular domain (2) is thought to be unimportant to monovalent cation selectivity and contributes to structural interactions across the tight junction cleft (Anderson and Van Itallie 2009; Piontek et al. 2008).

Studies of amino acid motifs within proteins of Zn^{2+} coordination sites involved in structural stability of proteins or in protein–protein interface sites have identified clusters of four cysteines (Auld 2009) or mixtures of four histidine/aspartate residues (Papageorgiou et al. 1995). Therefore, a possibility is that Zn^{2+} may bind to similar sites formed within the tight junction pore. The conserved cysteine residues in all claudin proteins could form such a coordination site within extracellular domain 1; this would physically occlude the pore while maintaining monovalent access to Asp68 to match the observed partial cation selectivity in the Zn^{2+} occluded pore. The claudin motif W-GLW-C-C is maintained in all claudins, but the functions remain unclear (Anderson and Van Itallie 2009). Mutation of either cysteine seems crucial for function (e.g., of claudin-5), but since the effects of mutation are not equivalent, intermolecular bonding or divalent ion coordination may be important. Given that a full divalent cation binding site requires residues from interacting claudin molecules across the junctional cleft, it seems possible that such divalent cation coordination might contribute to the mechanism of formation and stabilization of homotypic and heterotypic interactions between claudins (Zhong et al. 2010). A puzzling action of Zn^{2+} applied to both epithelial surfaces at the same time is the drop in epithelial resistance; perhaps full charge shielding of fixed negative sites within the pore when Zn^{2+} is available from both surfaces generates a high-conductance and nonselective state. Recent studies of alamethacin pores indicate that internally localized histidine residues may act as a Zn^{2+} binding site, resulting in extended open states of high conductance (Noshiro et al. 2010). In epithelial Na channels Zn^{2+} acts to block from an extracellular face; but if present concurrently at the cytosolic face of the channel, this relieves block and increases overall conductance (Amuzescu et al. 2003).

In conclusion, Zn^{2+}, at concentrations attained in therapeutic situations, increases barrier function in an archetypal leaky epithelium. The location of Zn^{2+} action is likely to be the paracellular junctional pore in which claudins determine the ion-selective properties. The present observations may be of significance to epidermis since claudin expression and formation of tight junctions are associated with maintaining the normal epidermal functional barrier (Brandner et al. 2002; Furuse et al. 2002).

Acknowledgments GC was supported by a Kidney Research UK Career Development Fellowship and JAW by a BBSRC studentship.

References

Amuzescu B, Segal A, Flonta ML, Simaels J, Van Driessche W (2003) Zinc is a voltage-dependent blocker of native and heterologously expressed epithelial Na^+ channels. Pflugers Arch 446:69–77

Anderson JM, Van Itallie CM (2009) Physiology and function of the tight junction. Cold Spring Harb Perspect Biol 1:a002584

Auld DS (2009) The ins and outs of biological zinc sites. Biometals 22:141–148

Balkovetz DF, Chumley P, Amlal H (2009) Downregulation of claudin-2 expression in renal epithelial cells by metabolic acidosis. Am J Physiol Renal Physiol 297:F604–F611

Blanchard A, Jeunemaitre X, Coudol P, Dechaux M, Froissart M, May A, Demontis R, Fournier A, Paillard M, Houillier P (2001) Paracellin-1 is critical for magnesium and calcium reabsorption in the human thick ascending limb of Henle. Kidney Int 59:2206–2215

Brandner JM, Kief S, Grund C, Rendl M, Houdek P, Kuhn C, Tschachler E, Franke WW, Moll I (2002) Organization and formation of the tight junction system in human epidermis and cultured keratinocytes. Eur J Cell Biol 81:253–263

Carr G, Haslam IS, Simmons NL (2006) Voltage dependence of transepithelial guanidine permeation across Caco-2 epithelia allows determination of the paracellular flux component. Pharm Res 23:540–548

Cereijido M, Robbins ES, Dolan WJ, Rotunno CA, Sabatini DD (1978) Polarized monolayers formed by epithelial cells on a permeable and translucent support. J Cell Biol 77:853–880

Colegio OR, Van Itallie C, Rahner C, Anderson JM (2003) Claudin extracellular domains determine paracellular charge selectivity and resistance but not tight junction fibril architecture. Am J Physiol Cell Physiol 284:C1346–C1354

Crane JK, Naeher TM, Shulgina I, Zhu CR, Boedeker EC (2007) Effect of zinc in enteropathogenic *Escherichia coli* infection. Infect Immun 75:5974–5984

Fromter E (1972) Route of passive ion movement through epithelium of *Necturus* gallbladder. J Membr Biol 8:259

Fromter E, Diamond J (1972) Route of passive ion permeation in epithelia. Nat New Biol 235:9

Furuse M, Furuse K, Sasaki H, Tsukita S (2001) Conversion of zonulae occludentes from tight to leaky strand type by introducing claudin-2 into Madin-Darby canine kidney I cells. J Cell Biol 153:263–272

Furuse M, Hata M, Furuse K, Yoshida Y, Haratake A, Sugitani Y, Noda T, Kubo A, Tsukita S (2002) Claudin-based tight junctions are crucial for the mammalian epidermal barrier: a lesson from claudin-1-deficient mice. J Cell Biol 156:1099–1111

Gitter AH, Bertog M, Schulzke J, Fromm M (1997) Measurement of paracellular epithelial conductivity by conductance scanning. Pflugers Arch 434:830–840

Hille B (1972) Permeability of sodium channel to metal cations in myelinated nerve. J Gen Physiol 59:637

Hoque KM, Sarker R, Guggino SE, Tse CM (2009) A new insight into pathophysiological mechanisms of zinc in diarrhea. Molecular structure and function of the tight junction: from basic mechanisms to clinical manifestations. Ann N Y Acad Sci 1165:279–284

Jacquillet G, Barbier O, Cougnon M, Tauc M, Namorado MC, Martin D, Reyes JL, Poujeol P (2006) Zinc protects renal function during cadmium intoxication in the rat. Am J Physiol Renal Physiol 290:F127–F137

Lansdown ABG, Mirastschijski U, Stubbs N, Scanlon E, Agren MS (2007) Zinc in wound healing: theoretical, experimental, and clinical aspects. Wound Repair Regen 15:2–16

Linley JE, Boese SH, Simmons NL, Gray MA (2009) A voltage-dependent Ca^{2+} influx pathway regulates the Ca^{2+}-dependent Cl^- conductance of renal IMCD-3 cells. J Membr Biol 230:57–68

Lo CM, Keese CR, Giaever I (1995) Impedance analysis of MDCK cells measured by electric cell-substrate impedance sensing. Biophys J 69:2800–2807

Lukacik M, Thomas RL, Aranda JV (2008) A meta-analysis of the effects of oral zinc in the treatment of acute and persistent diarrhea. Pediatrics 121:326–336

Moreno JH (1975) Blockage of gallbladder tight junction cation-selective channels by 2,4,6-triaminopyrimidinium (Tap). J Gen Physiol 66:97–115

Ng B, Barry PH (1995) The measurement of ionic conductivities and mobilities of certain less common organic ions needed for junction potential corrections in electrophysiology. J Neurosci Methods 56:37–41

Noshiro D, Asami K, Futaki S (2010) Metal-assisted channel stabilization: disposition of a single histidine on the N-terminus of alamethicin yields channels with extraordinarily long lifetimes. Biophys J 98:1801–1808

Papageorgiou AC, Acharya KR, Shapiro R, Passalacqua EF, Brehm RD, Tranter HS (1995) Crystal structure of the superantigen enterotoxin C2 from *Staphylococcus aureus* reveals a zinc-binding site. Structure 3:769–779

Piontek J, Winkler L, Wolburg H, Muller SL, Zuleger N, Piehl C, Wiesner B, Krause G, Blasig IE (2008) Formation of tight junction: determinants of homophilic interaction between classic claudins. FASEB J 22:146–158

Richardson JC, Scalera V, Simmons NL (1981) Identification of two strains of MDCK cells which resemble separate nephron tubule segments. Biochim Biophys Acta 673:26–36

Roselli M, Finamore A, Garaguso I, Britti MS, Mengheri E (2003) Zinc oxide protects cultured enterocytes from the damage induced by *Escherichia coli*. J Nutr 133:4077–4082

Roy SK, Behrens RH, Haider R, Akramuzzaman SM, Mahalanabis D, Wahed MA, Tomkins AM (1992) Impact of zinc supplementation on intestinal permeability in Bangladeshi children with acute diarrhea and persistent diarrhea syndrome. J Pediatr Gastroenterol Nutr 15:289–296

Sharir H, Zinger A, Nevo A, Sekler I, Hershfinkel M (2010) Zinc released from injured cells is acting via the Zn^{2+}-sensing receptor, ZnR, to trigger signaling leading to epithelial repair. J Biol Chem 285:26097–26106

Shen L, Weber CR, Turner JR (2008) The tight junction protein complex undergoes rapid and continuous molecular remodeling at steady state. J Cell Biol 181:683–695

Singh AB, Sugimoto K, Dhawan P, Harris RC (2007) Juxtacrine activation of EGFR regulates claudin expression and increases transepithelial resistance. Am J Physiol Cell Physiol 293:C1660–C1668

Stevenson BR, Anderson JM, Goodenough DA, Mooseker MS (1988) Tight junction structure and ZO-1 content are identical in two strains of Madin-Darby canine kidney cells which differ in transepithelial resistance. J Cell Biol 107:2401–2408

Sturniolo GC, Fries W, Mazzon E, Di Leo V, Barollo M, D'Inca R (2002) Effect of zinc supplementation on intestinal permeability in experimental colitis. J Lab Clin Med 139:311–315

Tang VW, Goodenough DA (2003) Paracellular ion channel at the tight junction. Biophys J 84:1660–1673

Tsien RW, Hess P, McCleskey EW, Rosenberg RL (1987) Calcium channels: mechanisms of selectivity, permeation, and block. Annu Rev Biophys Biophys Chem 16:265–290

Tsukita S, Furuse M (2002) Claudin-based barrier in simple and stratified cellular sheets. Curr Opin Cell Biol 14:531–536

Van Itallie CM, Fanning AS, Anderson JM (2003) Reversal of charge selectivity in cation or anion-selective epithelial lines by expression of different claudins. Am J Physiol Renal Physiol 285:F1078–F1084

Wright EM, Diamond JM (1968) Effects of pH and polyvalent cations on the selective permeability of gall-bladder epithelium to monovalent ions. Biochim Biophys Acta 163:57–74

Yu AS, Cheng MH, Angelow S, Gunzel D, Kanzawa SA, Schneeberger EE, Fromm M, Coalson RD (2009) Molecular basis for cation selectivity in claudin-2-based paracellular pores: identification of an electrostatic interaction site. J Gen Physiol 133:111–127

Zhong W, McClain CJ, Cave M, Kang YJ, Zhou Z (2010) The role of zinc deficiency in alcohol-induced intestinal barrier dysfunction. Am J Physiol Gastrointest Liver Physiol 298:G625–G633